



Dissimilar laser brazing of aluminum alloy and galvanized steel and defect control using interlayer

Tomo Ogura¹ · Reiko Wakazono¹ · Shotaro Yamashita¹ · Kazuyoshi Saida¹

Received: 20 August 2019 / Accepted: 21 January 2020 / Published online: 1 February 2020
© International Institute of Welding 2020

Abstract

The microstructure and tensile shear strength of the joint by laser brazing between dissimilar metals of aluminum alloy and galvanized (GA) steel were investigated. A blowhole was formed by zinc vaporization during laser brazing; the tensile shear strength was significantly affected not by intermetallic compounds (IMCs) at the filler metal/GA steel interface but by the blowhole. The vaporization of zinc was suppressed, and the blowhole was controlled by inserting a Ti interlayer. The joint strength was improved through the suppression of blowhole, the thermal deformation of the Ti interlayer, and the increase in brazed filler metal thickness by optimizing the brazing parameter. The hardness test revealed that fracture occurs preferentially in the brazed filler metal; however, as the brazed filler thickness increases, fracture begins to occur near the heat-affected zone of A5052 because the volume of filler metal increases. The maximum strength of the joint was 185 N/mm, which is about 73% of the joint efficiency to 254 N/mm of the A5052 base material, and the base material partly fractured.

Keywords Laser brazing · Aluminum alloys · Galvanized steel · Dissimilar materials · Interlayer

1 Introduction

In the automobile industry, multi-materialization is actively carried out, and as the main light weight material of automobiles, aluminum alloy is utilized from the viewpoint of weight reduction. As for the steel sheet, galvanized (GI; i.e., zinc coated) or galvanized (GA; i.e., alloyed zinc composed by zinc and iron intermetallic compounds (IMCs) coated) steel are the main materials used to achieve corrosion resistance. Therefore, dissimilar metal joining technology of aluminum alloy and GI or GA steel is important, and recently, some researchers have reported related welding studies [1–4]. However, owing to a joining method for aluminum alloy and steel in fusion welding methods such as arc welding, brittle IMCs are easily formed at the joining interface by

mutual diffusion between the aluminum alloy and steel. On the other hand, in the solid-phase joining method such as friction stir welding, very thin IMCs form at the interface, which attains high-quality joints [5–10]; however, there is a restriction from an equipment and a limit to application points. Laser brazing is characterized by easy control of material deterioration and deformation of the base material due to local heating, rapid heating, and rapid cooling of joints, with few restrictions on application points and high control of interface reaction layers [11–19].

In order to achieve successful laser brazing between dissimilar materials of aluminum alloy and GA steel, it is necessary to evaluate the microstructural and mechanical characteristics of the joint with various process parameters such as laser power, welding speed, and wire feeding speed. In the case of brazing a GI steel/aluminum alloy, the melting point of the coated pure zinc (419.5 °C) is lower than that of pure aluminum (660.3 °C), indicating that molten aluminum filler wire easily melts the coated zinc. The dissimilar laser brazing between GI steels and aluminum alloys has been reported or reviewed in the literature [20–22]. On the other hand, the surface of GA steel can also be coated with zinc and iron IMCs such as FeZn₃ and FeZn₈, which have melting points of 782 °C and 665 °C, respectively [23]. Therefore, the dissimilar laser brazing of aluminum alloy and GA steel is quite

Recommended for publication by Commission VII - Microjoining and Nanojoining

✉ Tomo Ogura
tomo.ogura@mapse.eng.osaka-u.ac.jp

¹ Division of Materials and Manufacturing Science, Graduate School of Engineering, Osaka University, 2-1 Yamadaoka, Suita, Osaka 575-0871, Japan

difficult because the GA coating composed of an alloyed zinc has a higher melting point than the aluminum filler wires and requires a high laser output to melt the plating. In addition, defects such as blowholes sometimes occur during the welding process; however, the examination of the defects generated during laser blazing is inadequate. The application of interlayers is a unique and useful technique for controlling the microstructures during welding and joining to obtain sound joints [9, 14, 24–28]. However, the application of an interlayer focused on the suppression of the pore formation has not yet been investigated.

The purpose of this study is to evaluate the joint properties of dissimilar laser brazing of aluminum alloy and GA steel and to optimize the laser brazing conditions using a Ti interlayer to suppress the pore defects.

2 Experimental procedure

The base metals for each test specimen were 1.0-mm-thick sheets of aluminum alloy A5052 and SPCC-GA steel. Al-Si flux-cored wire with a 1.2-mm diameter is used as the filler metal. The chemical compositions of these materials are shown in Table 1. The chemical composition of the GA coating obtained by EDS analysis and analyzed points are shown in Table 2 and Fig. 1, respectively.

After placing the A5052 sheet on top of the SPCC-GA sheet on a jig with a 15° inclination (Fig. 2a), laser brazing was applied to the lap weld using a fiber laser machine (IPG, YLS-6000 multi-mode fiber laser system), as shown in Fig. 2b. A jig with a 15° inclination to properly wet the molten filler metal to the root side of joint was described in our previous work [12]. Acetone was used to clean the surfaces of the base metals before laser brazing. The laser brazing conditions are listed in Table 3. Examination of the resulting microstructure and elemental analysis was performed using an optical microscope (OLYMPUS, DSX510) and a scanning electron microscope capable of energy-dispersive X-ray spectroscopy (JEOL, JCM-6000 plus). The mechanical properties of the brazed joint were evaluated at room temperature through tensile shear testing at a tension speed of 1.0 mm/min, as shown

Table 1 Chemical composition of the base metal and filler wire used in this study (mass%)

Mg	Si	Fe	Mn	Cr	Zn	Al	
A5052	2.57	0.09	0.29	0.01	0.17	0.01	Bal.
C	Mn	P	S				
SPCC	0.05	0.18	0.015	0.003			
Si	Fe	Cu	Mn	Mg	Zn	Al	
Al-Si flux-cored wire	1.88	0.10	0.01	<0.01	0.02	<0.01	Bal.

Table 2 EDS analysis of spots 1–5 in Fig. 1b (mol%)

Fe	Zn	Total	
1	10.3	89.7	100
2	15.3	84.8	100
3	14.8	85.2	100
4	23.2	76.8	100
5	26.7	73.3	100

in Fig. 2c. The joint strength (N/mm) was obtained by dividing the maximum force (N) by the specimen width (5 mm). The mean strength was calculated from three samples by excluding the maximum and minimum values from five samples. Hardness tests were performed with a load of 50 g for 10 s in order to investigate the hardness of each microstructure of laser-brazed joints using a micro-Vickers machine (SHIMAZU, HMV-G). The mean hardness was calculated from five samples.

3 Results and discussion

3.1 Brazing parameter and microstructures of A5052/GA steel laser-brazed joints

Figure 3 shows the relationship between laser power and V_f/V_w of the joints. The wire feeding speed was fixed at 20 mm/s, and laser brazing was performed by changing the laser power

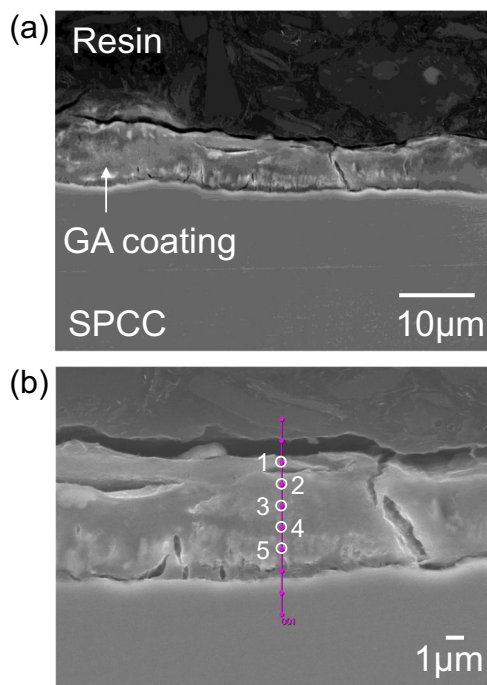
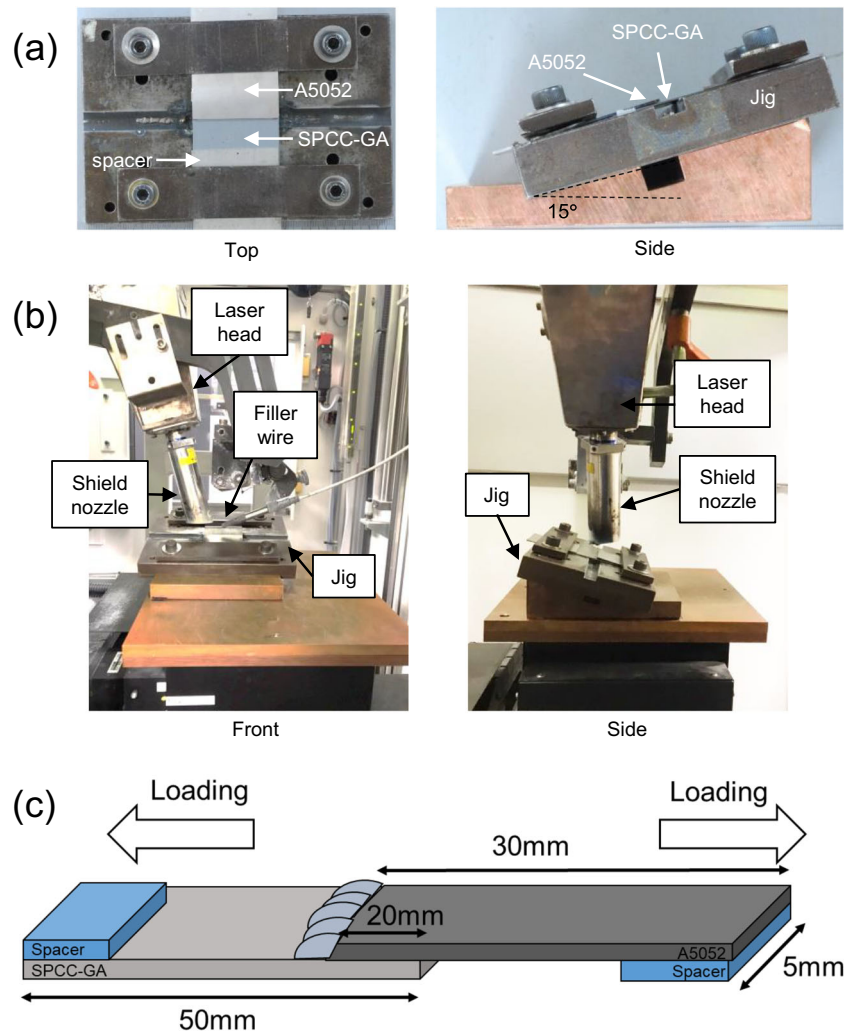


Fig. 1 a SEM image of GA steel and b magnified image and points analyzed via EDS

Fig. 2 **a** Clamping and tilting of specimens, **b** apparatus for laser brazing testing, and **c** schematic illustrations of specimen for tensile test



and V_f/V_w . After laser brazing, the weldable range was judged from the bead appearance. Insufficient heat caused insufficient melting of the wire under any conditions at a laser power of 1 kW, and bead appearance becomes unstable due to insufficient wire supply under conditions of 2 kW at $V_f/V_w = 3$ and 2 and 2.5 kW at $V_f/V_w = 4$. Burn through of the GA steel sheet occurred under conditions of 2 kW at $V_f/V_w = 7$, 3 kW at $V_f/V_w = 3, 6$ and over 3.5 kW. Good bead appearance was obtained under the conditions of 3 kW at $V_f/V_w = 4, 1.5$ to 3 kW at $V_f/V_w = 5$, and 1.5 to 2.5 kW at $V_f/V_w = 6$.

Table 3 Laser brazing conditions in this study

Processing parameter	Value
Beam power (W)	1000–4000
Defocusing diameter of beam (mm)	2–3
Traveling velocity, V_w (mm/s)	2.9, 3.3, 4.0, 5.0, 6.7
Wire feeding speed, V_f (mm/s)	20
Ar gas flow rate (l/min)	15

Figure 4 shows macrostructures of cross-sectional views of the A5052/GA steel laser-brazed joints. As the laser power increased, the bead width increased, and the bead toe angle

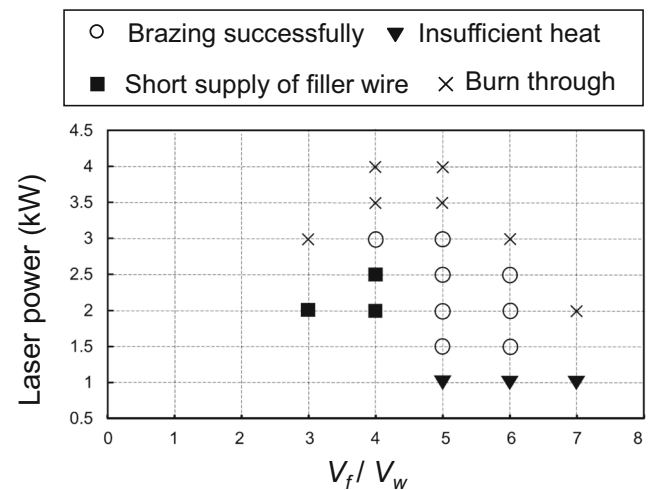


Fig. 3 Relationship between laser power and V_f/V_w

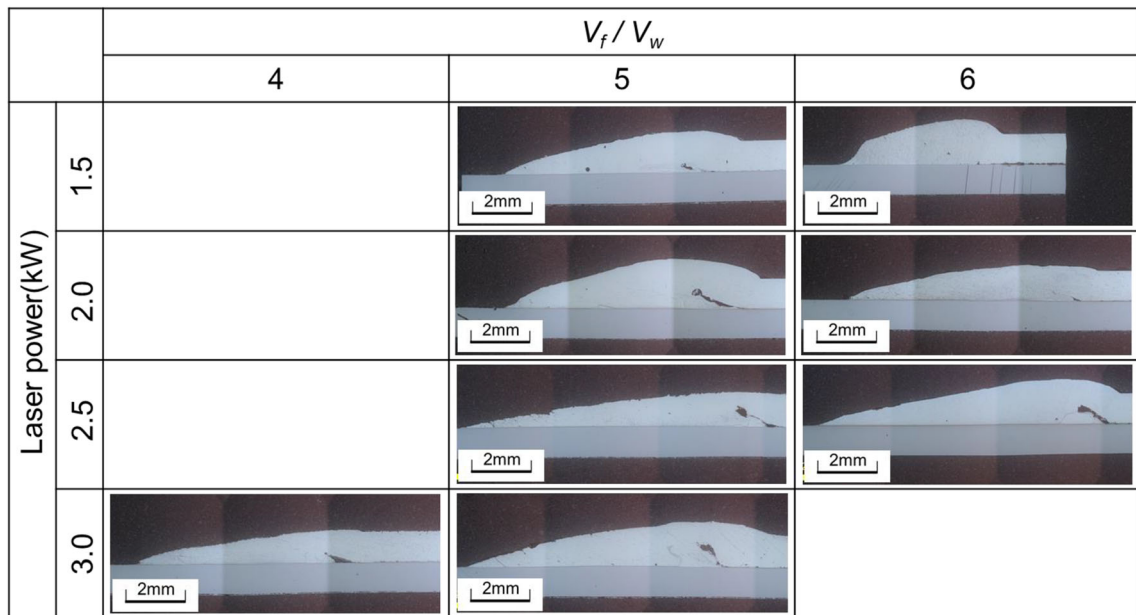
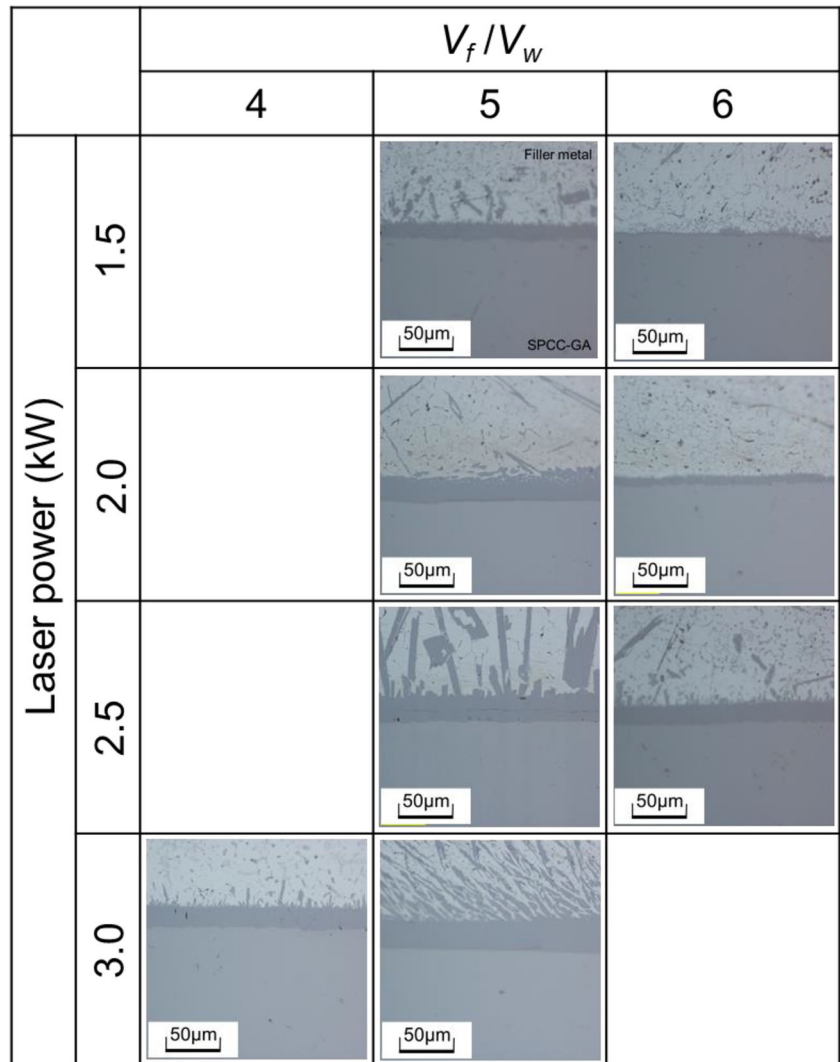


Fig. 4 Macrostructures of cross-sectional views of the A5052/GA steel laser-brazed joints

Fig. 5 Microstructures of the interface between filler metal and GA steel



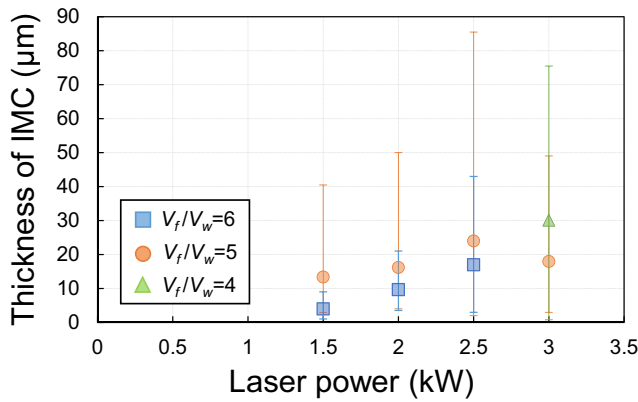


Fig. 6 Relationship between thickness of intermetallic compound and laser power and thermal history at the interface between titanium and A5052 produced by laser brazing at 800 W.

decreased, showing that the wettability of the brazing of the filler metal to the base material improved as the heat input increased. In addition, pore defects were also observed in the brazing material near the root of the lap joints. The IMCs formed at the filler metal/GA steel interface were observed. The results are shown in Fig. 5. The IMC thickness under each condition is shown in Fig. 6. It was found that the IMC became thicker as the laser power increased. The EDS analysis showed that the ratio of Al to Fe was approximately 3:1. Therefore, the IMC formed at the interface was found to be mainly Al_3Fe .

3.2 Tensile properties of A5052/GA steel laser-brazed joints

A tensile shear test was carried out to investigate the mechanical properties of the A5052/GA steel laser-brazed joints. The cross-sectional images after fracture are shown in Fig. 7. The

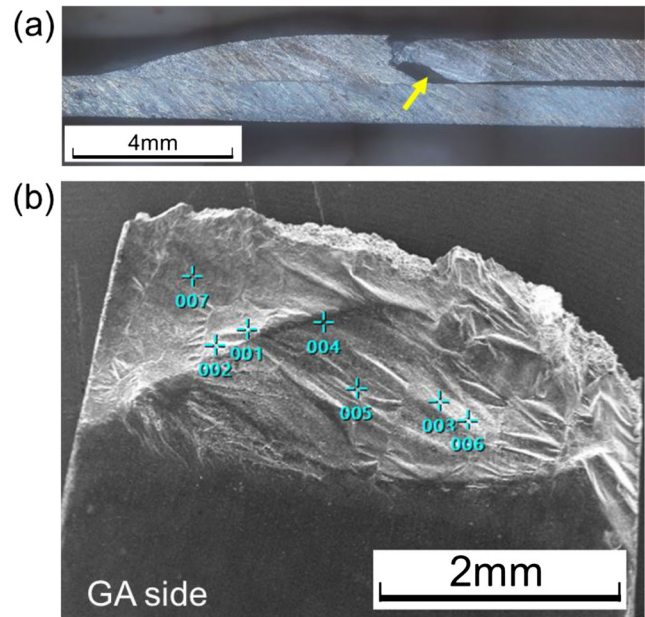


Fig. 8 a Macrostructures of cross-sectional views of the A5052/GA steel laser-brazed joints after tensile shear testing (2.5 kW, $V_f/V_w = 6$) and b analyzed points of EDS analysis

fractures occurred not only at the interface-formed IMC but over the entire brazed material surface, and most of them were fractures from pore defects.

In order to investigate pore defects, EDS analysis on pore defects after the tensile shear test was performed. The analyzed area was a pore defect at the GA steel side, which is indicated by the arrow shown in Fig. 8a and analyzed points and the corresponding results are shown in Fig. 8b and Table 4 respectively. A large amount of zinc was detected in the area where the analysis points 1, 2, 3, and 6 are located. The chemical compositions of the filler metal and the A5052 alloy used this study do not include zinc. Therefore, it is considered that

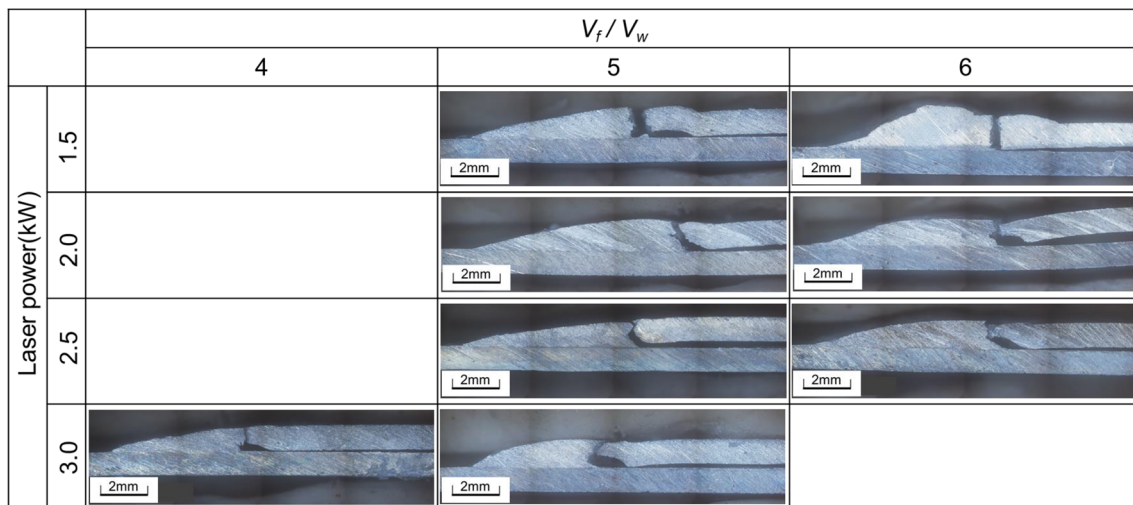


Fig. 7 Macrostructures of cross-sectional views of the A5052/GA steel laser-brazed joints after tensile shear testing

Table 4 EDS analysis of spots 1–7 in Fig. 8b (mol%)

Mg	Al	Si	Fe	Zn	Total	
1	5.2	55.6	0.6	0	38.6	100
2	5.9	53.6	6.6	1	32.9	100
3	10.8	79.3	6.3	0.2	3.4	100
4	4	91.6	3.7	0.5	0.2	100
5	6.4	86.6	6.1	0.4	0.5	100
6	23.5	56.1	11.5	0.9	8.2	100
7	3.1	89.2	6.8	1	0	100

the zinc component of the GA coating was vaporized and adhered to the pore. In order to clarify the vaporization of zinc during laser brazing, the thermal history was evaluated on the GA steel surface of the lap welded joint during laser brazing. A thermocouple was set on the GA steel surface during laser brazing, as shown in Fig. 9a. The result is shown in Fig. 9b. The maximum temperature was 917 °C at the lowest laser power (1.5 kW) under the joint conditions used in this study. This temperature result is well explained using the Fe-Zn phase diagram. The melting point of FeZn_3 IMC is up to 782 °C [23], and when laser brazing causes a temperature above this, a liquid phase of zinc is generated. Then, at 907 °C, the vaporization of zinc occurs because the vaporizing point of zinc is reached. Therefore, it is considered that the

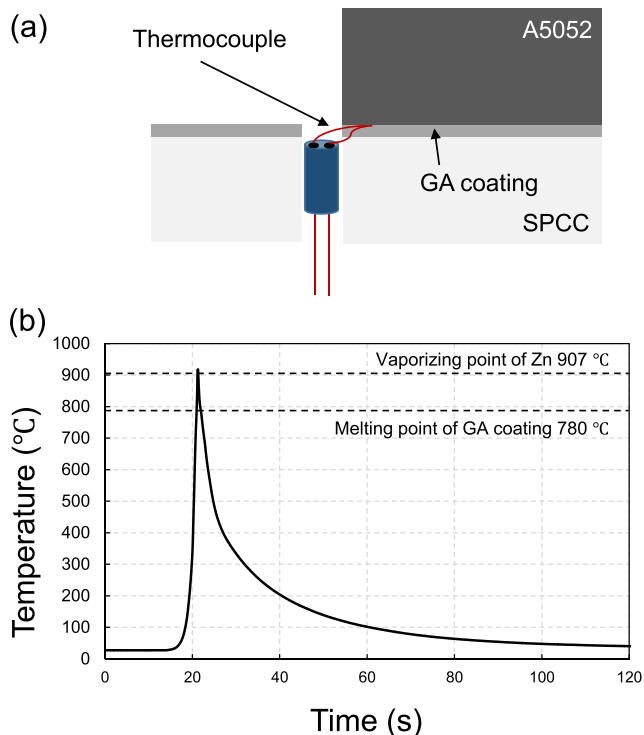


Fig. 9 a Schematic illustration of the placement of the thermocouple and b thermal history at the interface between A5052 and GA steel by laser brazing (1.5 kW, $V_f/V_w = 5$)

pore defect formed in this study is a blowhole due to the vaporization of zinc.

As shown in Fig. 7, the fracture occurred at a blowhole after the tensile shear testing, considering that not an IMC at the interface but a blowhole affects tensile shear strength. Therefore, tensile shear strength was evaluated by the residual thickness of the filler metal. The residual thickness of the filler metal was calculated by subtracting the thickness of the blowhole from the thickness of the filler metal, as shown in Fig. 10a. The mean residual thickness was obtained from three samples before tensile shear testing. The relationship between tensile shear strength and residual thickness of filler metal is shown in Fig. 10b, and the thickness of the IMC is shown in Fig. 10c. It was found that the tensile shear strength decreases as the residual brazing material thickness decreases, indicating that it is necessary to suppress a blowhole for the increase in the joint strength. In Fig. 10c, the tensile shear strength

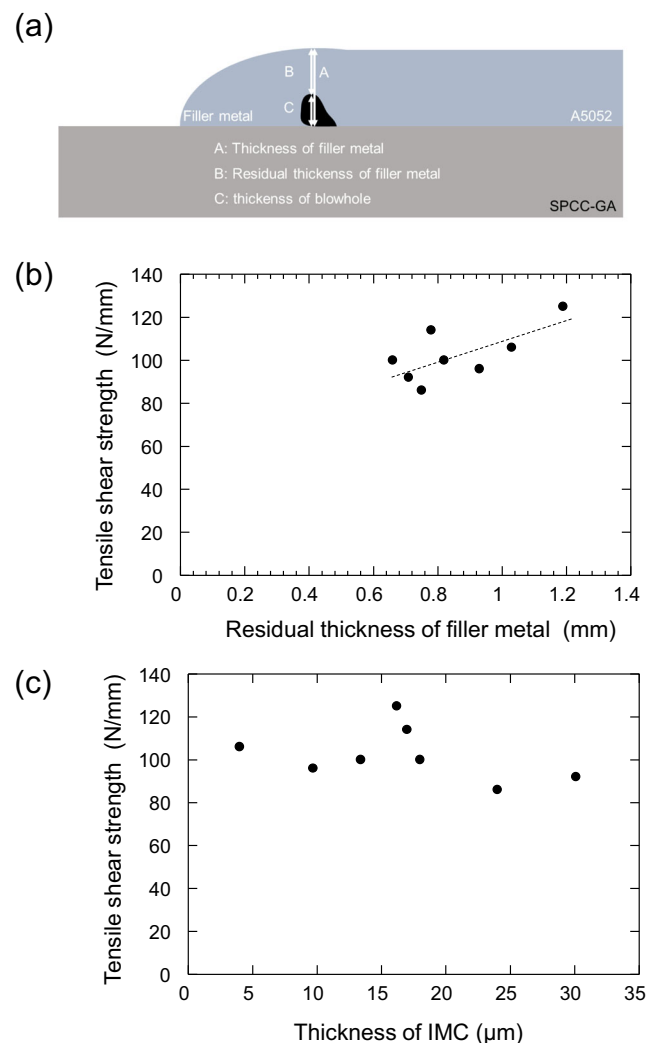


Fig. 10 a Definition of residual thickness of filler metal, b relationship between tensile shear strength and thickness of filler metal, and c relationship between tensile shear strength and thickness of the IMC

appears to decrease with the increasing thickness of the IMC; however, not an IMC at the interface but a blowhole affects the tensile shear strength because the fractures occurred not only at the IMC formed at the interface but also at pore defects, as shown in Fig. 7.

3.3 Effects of Ti interlayer on weldability of A5052/GA steel laser-brazed joints

In Sect. 3.2, the generation of a blowhole due to the vaporization of zinc during laser brazing was confirmed, which causes the decrease in the tensile strength. In this section, a Ti interlayer was inserted between the A5052 alloy and the GA steel to shield the heat, and the temperature of the GA steel surface during laser brazing could be suppressed below the boiling point of zinc. Ti has a high melting point (1668 °C) and is classified as a light metal, so it is suitable as an interlayer material in this study. Figure 11 shows that schematic illustration of a Ti interlayer. The thickness of a Ti interlayer was 50 μm . In order to investigate the optimum installation position of a Ti interlayer, laser brazing was performed by changing the position of the Ti interlayer from $x = -3$ to 3. Figure 12 shows the relationship between tensile shear strength and the position of a Ti interlayer (3 kW, $V_f/V_w = 5$). The result without a Ti interlayer was also shown. The maximum tensile shear strength of 148 N/mm was exhibited when the Ti interlayer position was -1 mm, and the strength increased above 100 N/mm without the interlayer. On the other hand, when the Ti interlayer position was 2 mm or more, the strength was lower than that without the interlayer. The cross-sectional images of the joints are shown in Fig. 13. A

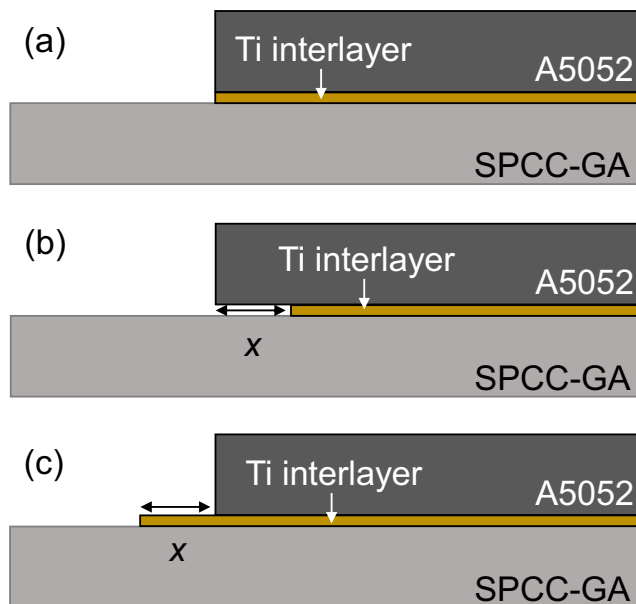


Fig. 11 Position of Ti interlayer a $x = 0$, b $x = -1, -2, -3$, c $x = 1, 2, 3$

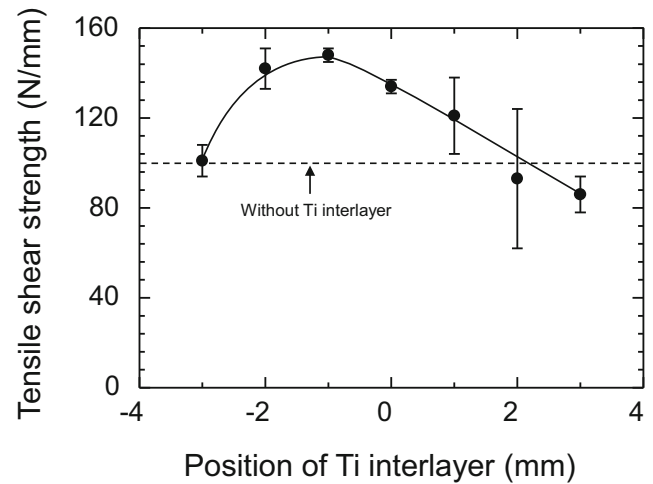


Fig. 12 Relationship between tensile shear strength and position of Ti interlayer (3 kW, $V_f/V_w = 5$)

blowhole was formed in the joint at $x = -3$ mm (Fig. 13a). Since the strength is the same as that without the interlayer, it was found that the effect of the interlayer is not at this position. On the other hand, the Ti interlayer was thermally deformed and penetrated into the brazing material in the joint of $x = -1$ and 2 mm (Fig. 13b and c) causing lower strength of the joint. In order to determine the presence or absence of vaporization of zinc, line analysis was performed by EDS at the bottom of the Ti interlayer at the joint of $x = -1$. The observed point is shown in Fig. 14. The EDS analysis results are summarized in Table 5. Alloyed zinc plating components considering FeZn_3 or FeZn_8 were detected at points 1–3 [23]. The chemical compositions and coating thickness were almost equal to those of the initial coating, as shown in Fig. 1 and Table 2. This indicates that the zinc component of the alloyed zinc plating in the bottom part of the Ti interlayer remained without being vaporized. That is, the vaporization of zinc was suppressed, and the blowhole was controlled by inserting the Ti interlayer. From the above, installing a Ti interlayer at -1 mm could be the optimal position.

Although the Ti interlayer suppressed the evaporation of zinc, thermal deformation of the Ti interlayer due to heat input was observed. Therefore, the laser power was reduced to suppress the thermal deformation of the Ti interlayer. In addition, the amount of the brazed filler metal (V_f/V_w) was increased to improve the joint strength by increasing the thickness of the brazed filler metal. The Ti interlayer position was fixed at -1 mm, and laser brazing was performed under the conditions of 2 kW, $V_f/V_w = 5$ and 2.5 kW, $V_f/V_w = 6$. The results are shown in Fig. 15. Compared with the maximum strength of the joint without the Ti interlayer (No. 1) and the joint with high laser power (No. 2), it showed tensile shear strength of 171 N/mm at 2 kW, $V_f/V_w = 5$, (No. 3) and 185 N/mm at 2.5 kW, $V_f/V_w = 6$ (No. 4). This strength is about 73% of joint efficiency to 254 N/mm of the A5052 base material. The

Fig. 13 Macrostructures of cross-sectional views of the A5052/GA steel laser-brazed joints with Ti interlayer **a** $x = -3$ mm, **b** $x = -1$ mm, and **c** $x = 2$ mm (3 kW, $V_f/V_w = 5$)

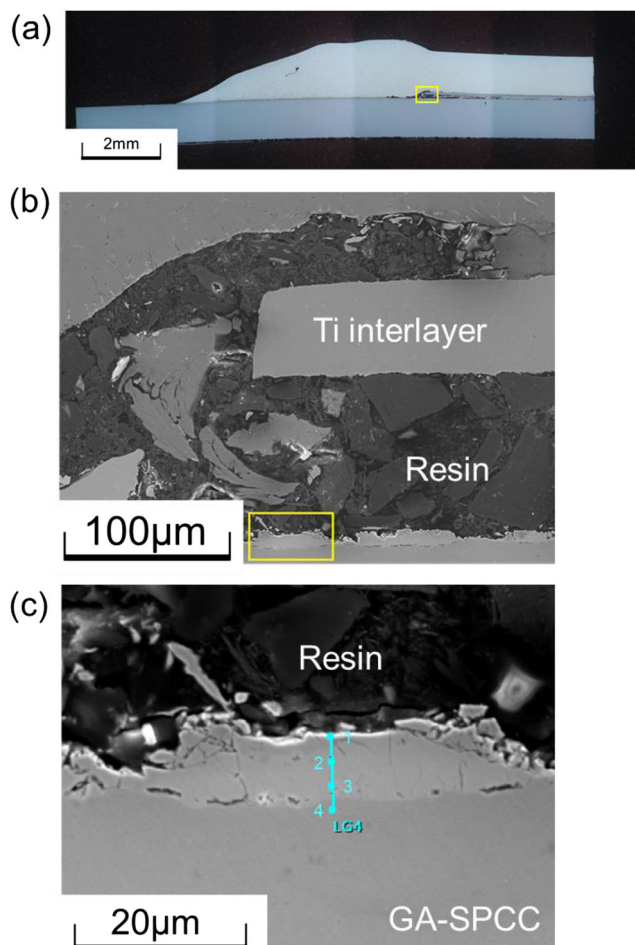
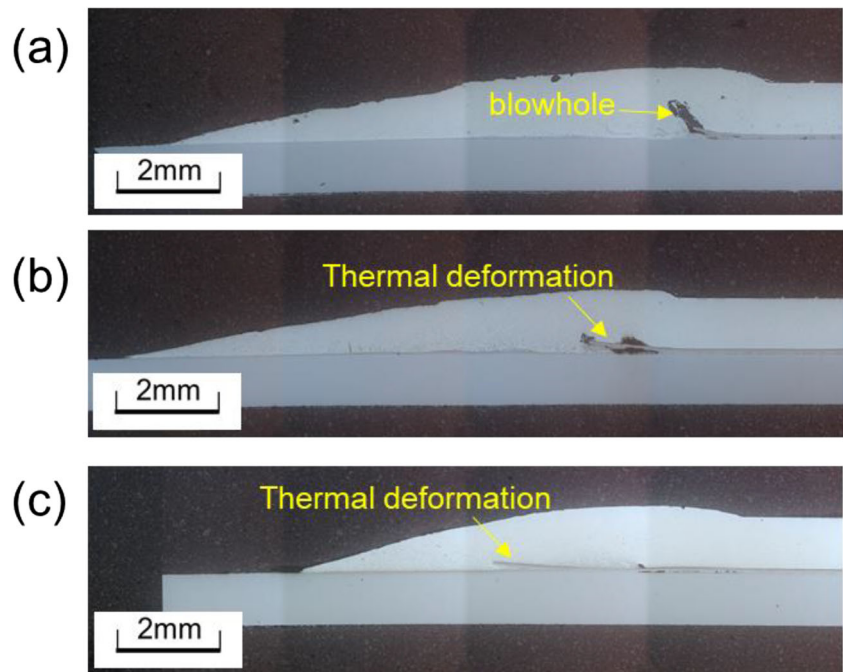


Fig. 14 **a** Macrostructure of the cross-sectional view of the A5052/GA steel laser-brazed joint with Ti interlayer, **b** magnified view of **a**, and **c** magnified view of **b** (2.5 kW, $V_f/V_w = 6$)

corresponding microstructures are shown in Fig. 16. One laser-brazed joint under the conditions of 2.5 kW and $V_f/V_w = 6$ showed base material fracture, indicating that joining was successfully achieved. From these results, it was found that tensile shear strength is improved by inserting a Ti interlayer and joining under optimized joining parameter conditions.

In order to investigate the hardness of each microstructure of the laser-brazed joint, hardness tests were performed on the brazed filler metal (A), the brazed filler metal/A5052 mixed (B), A5052 HAZ (C), and A5052 base metal (D) of the joint after laser brazing. The result is shown in Fig. 17. The average hardness of A-D is 54, 63, 60, and 69 HV. Therefore, it is considered that the fracture occurs preferentially in the brazed filler metal; however, as the brazed filler thickness increases, the joint cross-sectional area becomes larger and fracture occurs near the heat-affected zone of A5052. Therefore, it could be concluded that, by using the Ti interlayer and optimizing the brazing parameter, the joint strength was improved through suppressing the blowhole, controlling the thermal deformation of the Ti interlayer, and increasing the thickness of the brazed filler metal.

Table 5 EDS analysis of spots 1–4 in Fig. 14c (mol%)

	Fe	Zn	Total	
1	12.9	87.1	100	
2	12.6	87.4	100	
3	20.1	79.9	100	
4	98.9	1.1	100	

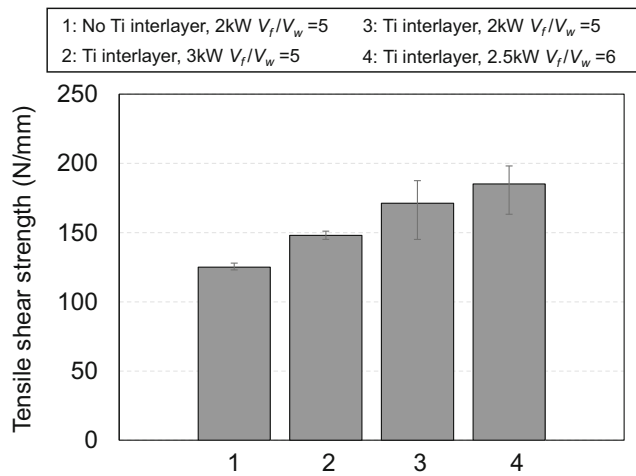


Fig. 15 Tensile shear strength of the A5052/GA steel laser-brazed joints under various conditions

4 Conclusion

The microstructures and mechanical properties of the joint were evaluated in the laser brazing between an aluminum alloy and GA steel. A Ti interlayer was used to increase the joint strength by suppressing the blowhole caused by zinc evaporation. The major findings were as follows:

- (1) Good bead appearance was attained under the conditions of 3 kW at $V_f/V_w=4$, 1.5 to 3 kW at $V_f/V_w=5$, and 1.5 to 2.5 kW at $V_f/V_w=6$ in this study.

Fig. 16 Macrostructure of the cross-sectional view of the A5052/GA steel laser-brazed joints with Ti interlayer and the fracture surface after tensile shear testing. **a** 2 kW, $V_f/V_w=5$, **b** 2.5 kW, $V_f/V_w=6$

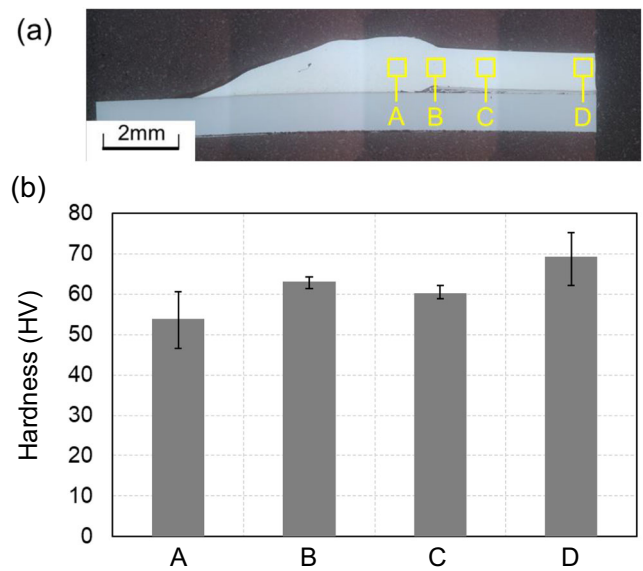
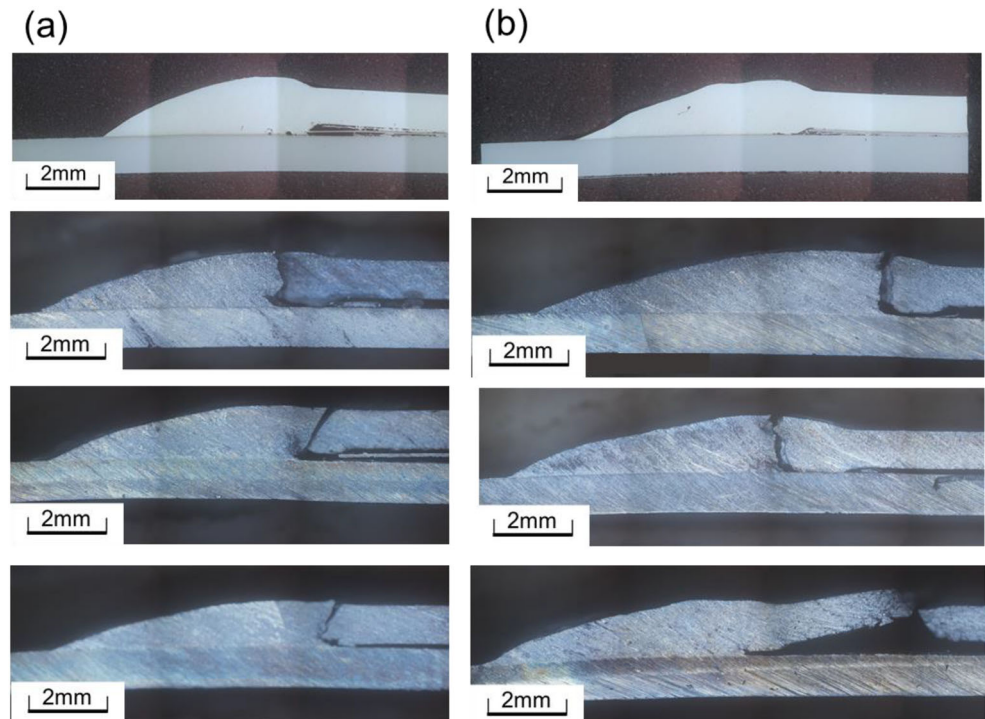


Fig. 17 **a** Macrostructure of the cross-sectional view and **b** hardness distribution of the A5052/GA steel laser-brazed joints with Ti interlayer at 2.5 kW, $V_f/V_w=6$. (A: brazed filler metal, B: brazed filler metal/A5052 mixed, C: A5052 HAZ, and D: A5052 base metal)

- (2) A blowhole was caused by zinc vaporization during laser brazing and it was found from the fracture position that the blowhole generation has a considerable influence on the joint strength.
- (3) The vaporization of zinc was suppressed, and the blowhole was controlled by inserting a Ti interlayer

- (4) The joint strength was improved through the suppression of blowhole, the thermal deformation of the Ti interlayer, and the increase in brazed filler metal thickness by optimizing the brazing parameter. The maximum strength of the joint was 185 N/mm, which is about 73% of joint efficiency to 254 N/mm of the A5052 base material, and the base material partly fractured.

Funding information This study was partial financially supported by The Light Metal Educational Foundation, Inc., Osaka, Japan. This study is based on results obtained from a project commissioned by the New Energy and Industrial Technology Development Organization (NEDO).

References

- Jia L, Shichun J, Yan S, Cong N, Junke C, Genzhe H (2015) Effects of zinc on the laser welding of an aluminum alloy and galvanized steel. *J Mater Process Technol* 224:49–59
- Dong H, Chena S, Song Y, Guo X, Zhang X, Sun Z (2016) Refilled friction stir spot welding of aluminum alloy to galvanized steel sheets. *Mater Des* 94:457–466
- Sakamura M, Ohishi K, Ota K, Takeyasu Y, Mizunari S, Fujii H (2016) Dissimilar spot welding of aluminum alloy and Galvannealed steel by metal flow. *Q J Jpn Weld Soc* 34-1:8–19 (in Japanese)
- Singh J, Arora KS, Shukla DK (2019) Dissimilar MIG-CMT weld-brazing of aluminium to steel: a review. *J Alloys Compd* 783:753–764
- Ogura T, Saito Y, Nishida T, Nishida H, Yoshida T, Omichi N, Fujimoto M, Hirose A (2012) Partitioning evaluation of mechanical properties and the interfacial microstructure in a friction stir welded aluminum alloy/stainless steel lap joint. *Scr Mater* 66:531–534
- Ogura T, Nishida T, Tanaka Y, Nishida H, Yoshikawa S, Fujimoto M, Hirose A (2013) Microscale evaluation of mechanical properties of a friction stir welded A6061 aluminium alloy/304 stainless steel dissimilar lap joint. *Sci Technol Weld Join* 18:108–113
- Nishida T, Ogura T, Nishida H, Fujimoto M, Takahashi M, Hirose A (2014) Formation of interfacial microstructure in a friction stir welded lap joint between aluminum alloy and stainless steel. *Sci Technol Weld Join* 19(7):609–616
- Ogura T, Hirose A (2016) Microstructural control of interface and mechanical properties in dissimilar metal joining between aluminum alloy and steel. *J Jpn Inst Light Met* 66(9):503–511 (in Japanese)
- Ogura T (2016) Dissimilar joining techniques between aluminum alloy and steel with controlled interfacial microstructures. *Q J Jpn Weld Soc* 85(6):593–598 (in Japanese)
- Hatano R, Ogura T, Matsuda T, Sano T, Hirose A (2018) Relationship between intermetallic compound layer thickness with deviation and interfacial strength for dissimilar joints of aluminum alloy and stainless steel. *Mater Sci Eng A* 735:361–366
- Saida K, Song W, Nishimoto K (2005) Diode laser brazing of aluminum alloy to steels with aluminum filler metals. *Sci Technol Weld Join* 10:227–235
- Saida K, Ohnishi H, Nishimoto K (2008) Fluxless laser brazing of aluminum alloy to galvanized steel using tandem beam - dissimilar laser brazing of aluminum alloy and steels. *J Jpn Welde Soc* 26-3: 235–241 (in Japanese)
- Saida K, Sakatani T, Song W, Nishimoto K (2009) Hot cracking in the laser braze joint of high strength stainless steel using gold brazing filler metal—prevention of hot cracking by controlling the thermal cycle. *Sci Technol Weld Join* 14:254–261
- Saida K, Ohnishi H, Nishimoto K (2015) Laser brazing of TiAl intermetallic compound using precious brazing filler metals. *Weld World* 59:9–22
- Yang J, Li Y, Zhang H, Guo W, Weckman D, Zhou N (2015) Dissimilar laser welding/brazing of 5754 aluminum alloy to DP 980 steel: mechanical properties and interfacial microstructure. *Metall Mater Trans A* 46A:5149–5157
- Ogura T, Yokochi T, Netsu S, Saida K (2016) Microstructure and mechanical properties in laser brazing of A5052/AZ31 dissimilar alloys. *Weld World* 60:1047–1054
- Ogura T, Netsu S, Yokochi T, Saida K (2017) Dissimilar metal joining of A5052 aluminum alloy and AZ31 magnesium alloy using laser brazing. *Mater Sci Forum* 879:2532–2536
- Ogura T, Netsu S, Ike K, Saida K (2018) Effects of titanium interlayer on dissimilar joining between aluminum alloy and magnesium alloy using laser brazing. *Q J Jpn Weld Soc* 36-4:247–252 (in Japanese)
- Yang J, Yu Z, Li Y, Zhang H, Zhou N (2018) Laser welding/brazing of 5182 aluminium alloy to ZEK100 magnesium alloy using a nickel interlayer. *Sci Technol Weld Join* 23:543–550
- Sierra G, Peyre P, Deschaux Beaume F, Stuart D, Fras G (2008) Galvanised steel to aluminium joining by laser and GTAW processes. *Mater Charact* 59:1705–1715
- Gatzen M, Radel T, Thomy C, Vollertsen F (2014) Wetting behavior of eutectic Al-Si droplets on zinc coated steel substrates. *J Mater Process Technol* 214:123–131
- Wang P, Chen X, Pan Q, Madigan B, Long J (2016) Laser welding dissimilar materials of aluminum to steel: an overview. *Int J Adv Manuf Technol* 87:3081–3090
- Kinzoku data book (2014) The Japan Institute of Metals, Maruzen, Tokyo, 509
- Kato K, Tokisue H (2004) Effect of insert metal on mechanical properties of friction welded 5052 aluminium alloy to pure titanium joint. *J Jpn Inst Light Met* 54:430–435 (in Japanese)
- Aritoshi M, Okita K, Ikeuchi K, Ushio M (1996) Friction welding of pure tungsten to oxygen free copper with intermediate layer. *Q J Jpn Weld Soc* 14:495–501
- Muralimohan CH, Ashifaq M, Ashiri R, Muthupandi V, Sivaprasad K (2016) Analysis and characterization of the role of Ni interlayer in the friction welding of titanium and 304 austenitic stainless steel. *Metall Mater Trans A* 47:347–359
- Madhusudhan RG, Venkata RP (2012) Role of nickel as an interlayer in dissimilar metal friction welding of maraging steel to low alloy steel. *J Mater Process Technol* 212:66–77
- Ogura T, Miyoshi K, Matsumura T, Imai T, Saida K (2019) Improvement of joint strength in dissimilar friction welding of Ti-6Al-4V alloy to type-718 nickel-based alloy using au-Ni interlayer. *Sci Technol Weld Join* 24:327–333

Publisher's note Springer Nature remains neutral with regard to jurisdictional claims in published maps and institutional affiliations.